

# Motor Current Signature Analysis for Deep Learning-Based Cross-Domain Fault Diagnosis

Journal Title  
XX(X):1-10  
©The Author(s) 2016  
Reprints and permission:  
sagepub.co.uk/journalsPermissions.nav  
DOI: 10.1177/ToBeAssigned  
www.sagepub.com/

SAGE

\*\*\*\*\*

## Abstract

In the recent years, intelligent data-driven fault diagnosis methods on gearboxes have been successfully developed and popularly applied in the industries. Currently, most of the machine learning techniques require that the training and testing data are from the same distribution. However, this assumption is difficult to be met in the real industries, since the gearbox operating conditions usually change in practice, which results in significant data distribution gap and diagnostic performance deteriorations in applying the learned knowledge on the new conditions. This paper proposes a deep learning-based domain adaptation method to address this issue. The raw current signals are directly used as the model inputs for diagnostics, which are easy to collect in the real industries and facilitate practical applications. The maximum mean discrepancy metric is introduced to the deep neural network, the optimization of which guarantees the extraction of generalized machinery health condition features across different operating conditions. The experiments on a real-world gearbox condition monitoring dataset validate the effectiveness of the proposed method, which offers a promising tool for cross-domain diagnosis in the real industries.

## Keywords

Fault diagnosis; deep learning; domain adaptation; gearbox; current signal.

## Introduction

In the past decades, rotating machines have been widely used in a large number of industries, such as manufacturing, aero-space industry, automotive *etc.* Gearbox is one of the key components in rotating machines for delivering torque and offering speed conversions. Effective and timely fault diagnosis of gearbox is of great importance in the real industries, which can optimize maintenance schedule, enhance operational safety and reduce economic costs<sup>1,2</sup>.

Traditionally, many model-based signal processing methods have been used for the fault signal analysis of gearbox<sup>3</sup>. While effective diagnosis results have been obtained, the model-based approaches generally rely on good expert knowledge, and require much human labor on model development. Therefore, they are less efficient for applications in the real industrial scenarios. On the other hand, the global movements towards smart manufacturing and cyber-physical systems have paved the way for massive data access enabling development and realization of data-driven methods in fault detection and diagnosis of mechanical systems<sup>4,5,6</sup>. In general, high diagnosis accuracy and fast implementation can be achieved<sup>7</sup>. Furthermore, little prior expertise on signal processing and dynamics model of gearbox is generally required, which largely facilitates the industrial applications.

In the literature, the popular data-driven methods include artificial neural networks (ANN), random forest (RF), support vector machines (SVM) and so forth. Recently, deep learning has been emerging as a highly effective algorithm for data processing, which is promising to further improve the performance of the existing data-driven approaches<sup>8</sup>. Basically, the deep learning methods are capable of efficiently capturing the underlying relationship

between input and output data, through multiple linear and non-linear data transformations<sup>9</sup>. Specifically, with respect to fault diagnosis problems, the machinery health states can be well predicted using the collected condition monitoring data, despite the high dimensions of the signals<sup>10,11</sup>.

Authors in<sup>12</sup> proposed using convolutional neural network (CNN) for gearbox fault diagnosis and achieved a significantly better classification accuracy compared to the classical machine learning methods. A fault diagnosis method for wind turbine gearbox based on stacked auto-encoder and multi-class SVM was proposed in<sup>13</sup>. A Deep Belief Network fault diagnosis method based on manually extracted time and frequency domain features was proposed in<sup>14</sup> for gearbox and bearing applications. These studies emphasize the significant improvement in gearbox fault diagnosis performance by using deep learning based methods compared to the conventional data-driven methodologies. It should be pointed out that while promising diagnosis performance has been obtained using deep learning, the main assumption lies in that the training and testing data are supposed to be from the same distribution. That means the labeled training data and unlabeled testing data should be collected in the similar operating conditions of gearbox. However, the working

<sup>1</sup>Department of Mechanical and Materials Engineering, University of Cincinnati, Cincinnati 45221, USA

<sup>2</sup>Key Laboratory of Vibration and Control of Aero-Propulsion System Ministry of Education, Northeastern University, Shenyang 110819, China

## Corresponding author:

Xiang Li, University of Cincinnati, USA

Email: ll5xi@ucmail.uc.edu

scenarios such as load, rotating speeds *etc.* usually change in different practical industrial tasks. That results in significant distribution discrepancy between training and testing data, which deteriorates the data-driven model generalization performance<sup>15</sup>.

In order to address this problem, transfer learning algorithms have been proposed in the recent years<sup>16</sup>, which aim to generalize the data-driven knowledge learned from the training condition, denoted as source domain, to the testing condition, denoted as target domain. Specifically, the domain adaptation (DA) techniques have been popularly developed in the fault diagnosis field<sup>17,18</sup>, which assume the training and testing data share the same label space. That is consistent with the machinery health condition identification problems<sup>19</sup>. The domain-invariant features across different conditions are expected to be learned with the domain adaptation methods, and stronger model generalization ability can be achieved.

A framework for gearbox domain adaptation was proposed in<sup>20</sup> based on deep neural network, where only the source domain data and healthy data from the target domain were used to accomplish the DA tasks. In<sup>21</sup>, a DA approach for fault diagnosis of low-speed bearing was proposed. The authors used acoustic spectral imaging technique to convert time-domain acoustic emission signal to representative images for different health conditions. These images were used in a DA model for predicting labels of target domain dataset. A deep CNN-based DA method for gearbox fault diagnosis was proposed in<sup>22</sup> based on vibration signal. In their approach, the raw time-domain vibration signal was converted to gray-scale images and used as input to the CNN model. The authors firstly trained a CNN model on the source dataset and then fine-tuned it using the target domain samples. In general, the deep learning-based domain adaptation methods have shown great potential in bridging the domain gap in different working conditions<sup>23,24</sup>.

In the current literature, the machinery vibration data are mostly focused for fault diagnosis<sup>25</sup>, since the vibration signal is representative of the behavior of periodic events in the gearbox and it is expected the behavior of the gearbox would change in case of any kind of mechanical abnormality. For different kinds of signals, the application of the torque measurement has been seldomly investigated. The authors in<sup>3</sup> discussed torsional vibration analysis as a potential approach for fault diagnosis in fixed shaft gearboxes. Using torque signal in fault diagnosis of planetary gearboxes was discussed in<sup>26</sup> and the authors proposed a diagnosis method based on the demodulated spectra of amplitude envelope and instantaneous frequency. The study by Qiao *et al.*<sup>27</sup> on wind turbine mechanical components pointed out the usefulness of the torque signal in detecting gearbox faults.

Furthermore, Mohanty *et al.*<sup>28</sup> stated that the current signal of the induction motor driving the gearbox is useful for the fault diagnosis investigations, and the motor current signature analysis (MCSA) can be largely improved using the proposed demodulation method. The effectiveness of MCSA in rotating machinery fault diagnosis problems was also validated in<sup>29,30</sup>. Therefore, it is feasible and promising to explore the current signals for gearbox health identification, which are easy to collect in the real industries. However, it should be pointed out that the existing methods

are mostly complicated and require sophisticated domain knowledge on gearbox modeling and signal processing skills, which are difficult to be implemented in different applications.

This paper proposes a deep learning-based domain adaptation method for the gearbox fault diagnosis. An end-to-end diagnostic framework is built, which takes the raw collected data as input and directly outputs the results. The current signals are investigated in this study, which are generally easier to collect than the popular vibration data in the real industrial scenarios. The maximum mean discrepancy metric is introduced to measure and minimize the data distribution distance between different domains, and the generalized diagnostic features of different machinery health conditions can be extracted. Experiments on real-world gearbox datasets are implemented for validations, and the proposed method is capable of effectively diagnosing gearbox faults across different operating scenarios.

The remainder of this paper starts with the preliminaries in Section . The proposed fault diagnosis method is shown in Section , and experimentally validated and investigated in Section . We close the paper with conclusions in Section .

## Preliminaries

### *Deep Convolutional Neural Network*

In the past years, deep learning also denoted as deep neural network has achieved great success in different applications. Besides the basic multi-layer perceptron (MLP) structure, the convolutional neural network (CNN) architecture has been more efficient on feature extraction and the high-dimensional machinery data can be well processed<sup>9</sup>.

Basically, multiple convolutional layers are stacked in the CNN structure to model the relationship between input and output. Specifically, the one-dimensional CNN is adopted in this study, which is well suited to process the measurement signals of gearboxes.

Together with convolutional operations, pooling is usually implemented after the convolutional layers. The averaging-pooling and max-pooling operations are popularly adopted, which are able to learn the average and maximum values from the local data respectively. In this way, the most significant features can be extracted and the data dimensions can be reduced, which increases the computing efficiency of deep learning. By exploiting the convolutional and pooling operations, the high-level features from raw data can be obtained, and they can be used for the final task afterwards, i.e. machinery fault diagnosis. Readers are referred to<sup>9,31</sup> for more descriptions of CNN.

### *Domain Adaptation*

To bridge the gap between different data distributions on machine learning, transfer learning techniques have been successfully developed and widely used in the applications<sup>32</sup>. Specifically, the domain adaptation method in transfer learning has been receiving increasing attention in the fault diagnosis studies, since the machinery health condition label spaces are usually identical. In general, the domain adaptation approaches aim to learn domain-invariant features

from different conditions, that facilitates the fault diagnostic knowledge generalize in different cases<sup>16</sup>.

In this paper, the maximum mean discrepancy (MMD) metric is adopted, which measures the distance between the distributions of source and target domains. The optimization of MMD is able to achieve domain fusion in the high-level representation sub-space in deep neural networks, and thus extract generalized features for diagnosis<sup>18</sup>.

The MMD metric is defined as the squared distance between the kernel embeddings of data marginal distributions in the reproducing kernel Hilbert space (RKHS) as,

$$\text{MMD}_k(P, Q) \triangleq \|\mathbf{E}_P[\phi(\mathbf{x}^s)] - \mathbf{E}_Q[\phi(\mathbf{x}^t)]\|_{\mathcal{H}_k}^2, \quad (1)$$

where  $\mathcal{H}_k$  denotes the RKHS endowed with the characteristic kernel  $k$ .  $P$  and  $Q$  represent the distributions of the source and target domains, respectively.

Based on the current understanding of MMD<sup>33</sup>, kernel choice is one of the key factors in domain adaptation, since different kernels can embed the probability distributions in different RKHSs and different orders of the statistics are explored. Therefore, multiple kernels in MMD are employed in this paper to leverage different kernels and achieve improved performance. In the implementations,  $N_k$  RBF kernels are used as<sup>34</sup>,

$$k(\mathbf{x}^s, \mathbf{x}^t) = \sum_{i=1}^{N_k} k_{\sigma_i}(\mathbf{x}^s, \mathbf{x}^t), \quad (2)$$

where  $k_{\sigma_i}$  denotes a Gaussian kernel with bandwidth coefficient  $\sigma_i$ . In this study, three kernels are adopted, and the bandwidth parameters are selected as 2, 4 and 8.

## Proposed Fault Diagnosis Method

The proposed method is described in Figure 1 and consists of four individual steps. In each step, the key functionalities are presented and discussed in detail.

### Data Partitioning

In the first phase, the raw time-domain sensor data collected from a gearbox is partitioned into two sets (a) source domain data (labeled data) and (b) target domain data (unlabeled data). The target domain data is also further partitioned into training and testing sets, where one of the unlabeled subset is used in training the CNN model and the other subset is used for testing the trained model.

### Data Modeling

There are two major steps for modeling the data prior to training the diagnosis model, which are presented as follows.

**Data augmentation** In order to increase the number of training samples, a windowing method has been used. As depicted in Figure 2, a window with a fixed sample size moves over a time series signal and generates multiple samples. For example, a signal with 1000,000 points can provide the 191 training samples with length 50,000 when the shift size is 5000 points.

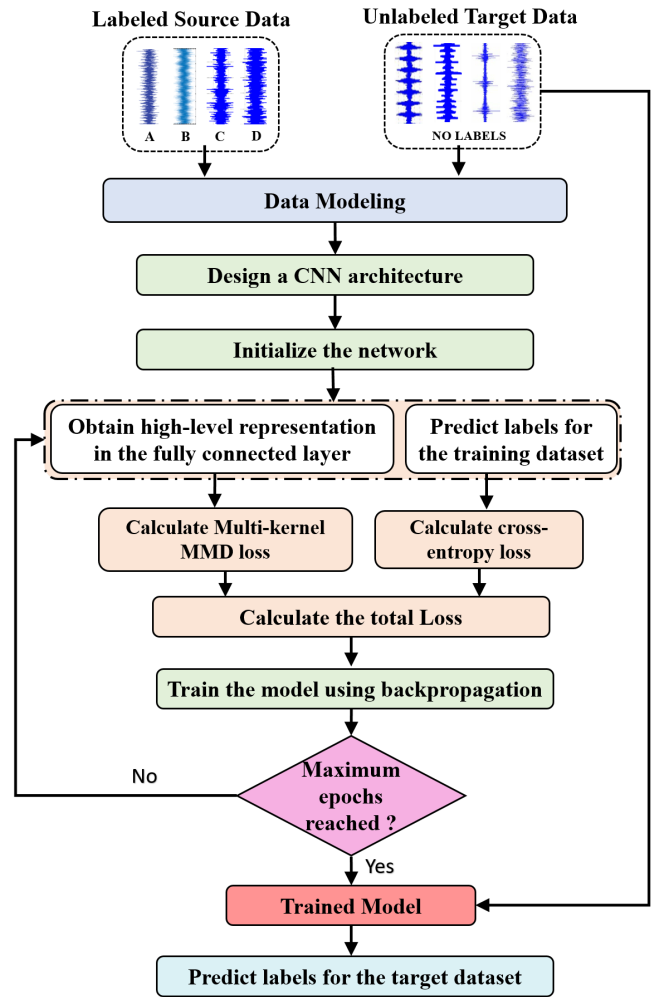


Figure 1. Flowchart of the proposed fault diagnosis method.

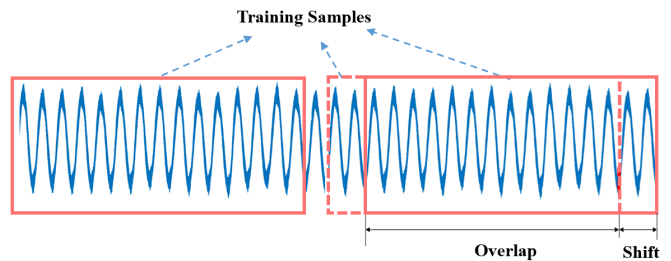


Figure 2. data augmentation with overlap.

**Fast Fourier Transform (FFT)** In order to eliminate the impact of the supply line frequency, the FFT technique is applied to each sample generated from the augmentation process. It is expected that fault signatures appear as sidebands around the supply line frequency (or running frequency) in the FFT spectrum<sup>35</sup>. All samples after FFT are directly used in the deep learning model for feature learning and fault diagnosis.

### Deep Learning Model Formulation

For the network optimization, two terms are generally included in the objective, i.e. source-domain classification loss and domain discrepancy loss. First, following the typical

machine learning paradigm, the empirical health condition identification errors on the source domain are supposed to be minimized, and the cross-entropy loss function  $L_s$  is adopted in this study, which is defined as,

$$\min L_s = -\frac{1}{n_s} \sum_{i=1}^{n_s} \sum_{j=1}^{N_c} 1\{y_i = j\} \log \frac{e^{x_{i,j}^s}}{\sum_{m=1}^{N_c} e^{x_{i,m}^s}}, \quad (3)$$

where  $n_s$  denotes the number of the source-domain training samples.  $x_{i,j}^s$  is the  $j$ -th element of network output vector, taking as input the  $i$ -th labeled source-domain sample, and  $y_i$  is the label of the  $i$ -th source-domain sample.  $N_c$  represents the number of the concerned machinery health conditions.

Besides the basic supervised learning part, the source and target domain discrepancy should be minimized, and the MMD metric is adopted to measure and optimize the domain gap in this study as described in Section . Specifically, the MMD loss  $L_d$  is defined as,

$$\min L_d = \text{MMD}_k(P_S, P_T), \quad (4)$$

where  $P_S$  and  $P_T$  denote the distributions of the high-level representations of the source and target-domain data respectively in the last fully-connected layer of the network.

In summary, the losses in Equations (3) and (4) can be combined, and the final optimization objective  $L_{opt}$  can be expressed as,

$$\min L_{opt} = L_s + L_d, \quad (5)$$

In the model training process, the network parameters can be optimized in each epoch as,

$$\theta \leftarrow \theta - \delta \left( \frac{\partial L_s}{\partial \theta} + \alpha \frac{\partial L_d}{\partial \theta} \right), \quad (6)$$

where  $\theta$  represents the network parameters, and  $\delta$  denotes the learning rate.

### Model Testing

In this step, the unlabeled testing target-domain data are used for fault diagnosis and performance of the proposed method is reported.

## Experimental Study

### Test Rig

A validation study has been conducted on a dataset acquired from a gearbox prognostic simulator (GPS) built by the Spectra Quest Company, as is shown Figure 3. Two confronted electrical motors are used in the test rig; one motor is used for drive and the other one for resistance/load. Both motors are three-phase induction motors with 10 Hp and two pair of poles. A current sensor (HTA 100) was installed on the drive motor and was used in our analysis for fault diagnosis. The data was recorded using a computer with a National Instruments acquisition card (NI 4472 series) at a sampling rate of 50 ks/sec.

The monitored gearbox is composed of four spur gears (Figure 4). The first gear, as it comes from the motor that drives the test bench, has 32 teeth. It is the one substituted by gears in different health states, leaving the rest unchanged. It is followed by a gear with 80 teeth. In the same axle, a gear

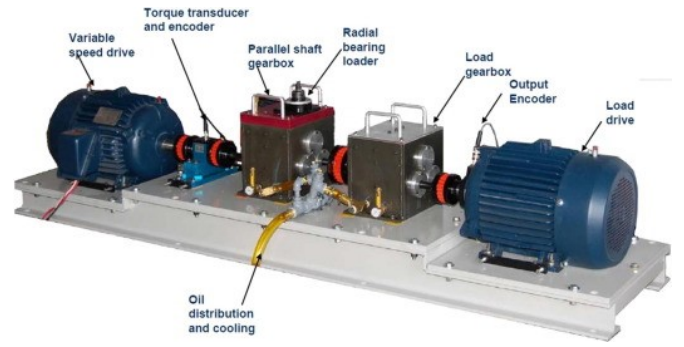


Figure 3. The experimental setup of the test rig.

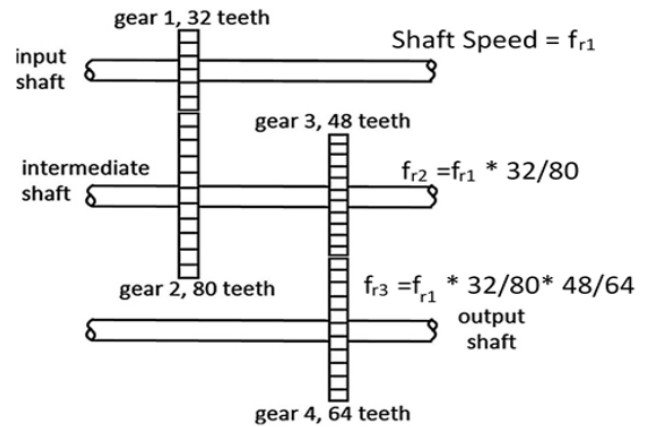


Figure 4. Illustration of the gear disposition inside the experimental gearbox.

Table 1. Experimental details.

Experiment Number	Load	Speed (rpm)
1	0%	1500
2	40%	1500
3	80%	1500
4	100%	1500

with 48 teeth is found, connected to a gear with 64 teeth, resulting in a global transmission relationship of 3.33.

In this study, the torque load applied to the gearbox was gradually increased by 40%, 80%, and 100%. In each load, the operational speed was kept constant at 1500 rpm and each run was repeated 15 times to reduce the impact of randomness and uncertainties. Table 1 summarizes the experimental studies and a comparison between raw motor current measurements and the corresponding FFT spectra for different loads and in healthy condition is given in Figure 5. Accordingly, by increasing the load condition, amplitude of raw current signal and FFT spectrum increase significantly.

Figure 6 shows the five health conditions examined in this paper and the impact of FFT analysis in distinguishing different faults at 0% load is given in Figure 7. As shown, raw motor current measurements do not show significant differences between different health conditions, however, they are clearly distinguishable from the FFT spectrum.

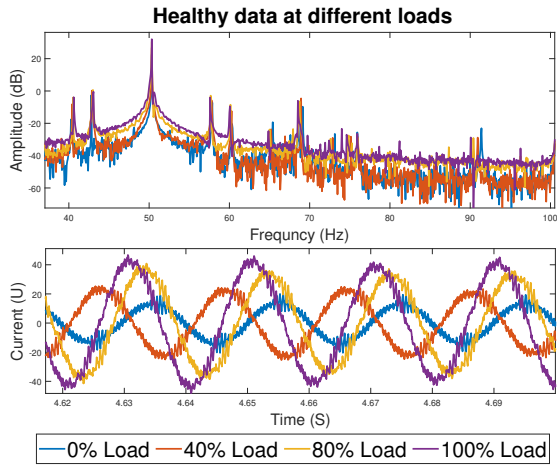


**Figure 5.** Comparison between healthy data at different load conditions.

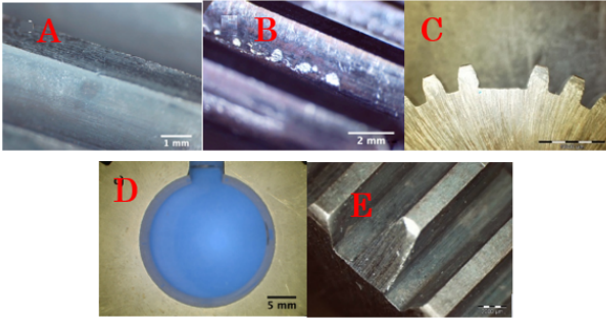


**Figure 6.** Five health conditions examined in this paper. The fault diagnosis tasks are the same at different speeds which indicates the class categories are shared.

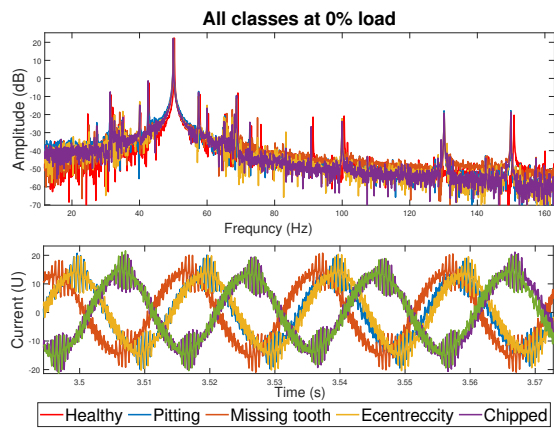


**Figure 7.** Different health conditions indicated in raw time domain and frequency spectrum.

The proposed method is tested for six transfer tasks, i.e.  $T_{1-2}$ ,  $T_{1-3}$ ,  $T_{1-4}$ ,  $T_{4-3}$ ,  $T_{4-2}$  and  $T_{4-1}$ . The subscripts indicate transfer tasks between different experiments. For example, the task  $T_{1-2}$  denotes using the data from experiment #1 as the source for supervised model training and the unlabeled data from the experiment #2 for testing.

**Table 2.** Data segmentation for different transfer tasks.

Transfer Task	Source Sample Number	Target Sample Number
$T_{1-2}$	$5 \times N_{source}$	$5 \times N_{target}$
$T_{1-3}$	$5 \times N_{source}$	$5 \times N_{target}$
$T_{1-4}$	$5 \times N_{source}$	$5 \times N_{target}$
$T_{4-3}$	$5 \times N_{source}$	$5 \times N_{target}$
$T_{4-2}$	$5 \times N_{source}$	$5 \times N_{target}$
$T_{4-1}$	$5 \times N_{source}$	$5 \times N_{target}$

These tasks show the effectiveness of the proposed method for model transferability in different operation situations. A summary of data segmentation for different tasks is given in Table 2.  $N_{source}$  and  $N_{target}$  represent the number of samples from each class of source and target domain datasets respectively. All experiments are performed on a PC with 16-GB RAM, Core i5 CPU, and NVIDIA GeForce TX 2080 Ti. The programming is done in Tensorflow and GPU computing is used to reduce the model training time.

### Model Architecture Design

As shown in Figure 8, the first step is to design a CNN architecture and tune the network parameters. In this study, a stack of four convolutional and pooling layers and a max-pooling layer are used for model training.

The impact of filter size ( $F_s$ ) and filter number ( $N_f$ ) on the cross domain diagnosis performance and for task  $T_{1-2}$  is shown in Figure 9. Generally, a larger value for  $N_f$  and  $F_s$  leads to a higher diagnosis accuracy, but this improvement by larger values is relatively limited. Moreover, by increasing  $N_f$  and  $F_s$ , the training time increases significantly. Therefore,  $N_f = F_s = 20$  was selected for the final model.

Batch size ( $N_b$ ) is another tuning parameter that may significantly affect the diagnosis accuracy. For our dataset, selection of low batch size leads to the worst diagnosis results and a too large batch size would create a big cumulative descent in updating the parameters especially when MMD loss is integrated in the model and therefore the prediction accuracy drops for too large batch sizes. Therefore, it is important to choose a reasonable tradeoff value for  $N_b$ . Consequently,  $N_b = 64$  was selected for the final diagnosis model.

The confusion matrix corresponding to the final diagnosis results in task  $T_{1-2}$  is illustrated in Figure 10. It is observed that only two classes ‘eccentricity’ and ‘missing tooth’ are slightly misclassified and all other classes are precisely classified.

### Results and comparison

In this section, different implementations are used to evaluate the performance of the proposed method and comparison with the latest related works is also presented.

**Effects of training sample size** Performance of the final model in different tasks, i.e.  $T_{1-2}$ ,  $T_{1-3}$ ,  $T_{1-4}$ ,  $T_{4-3}$ ,  $T_{4-2}$  and  $T_{4-1}$  and for different source domain sample size,  $N_{source}$ , is illustrated in Figure 11. In this study the number of target samples,  $N_{target}$ , is kept constant at 300. With increasing  $N_{source}$ , the testing accuracy increases and

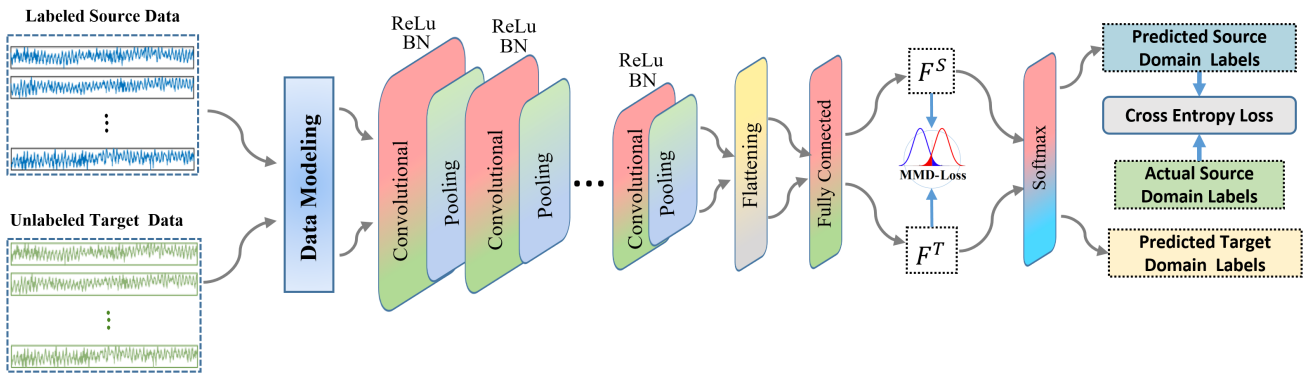


Figure 8. The proposed deep neural network architecture.

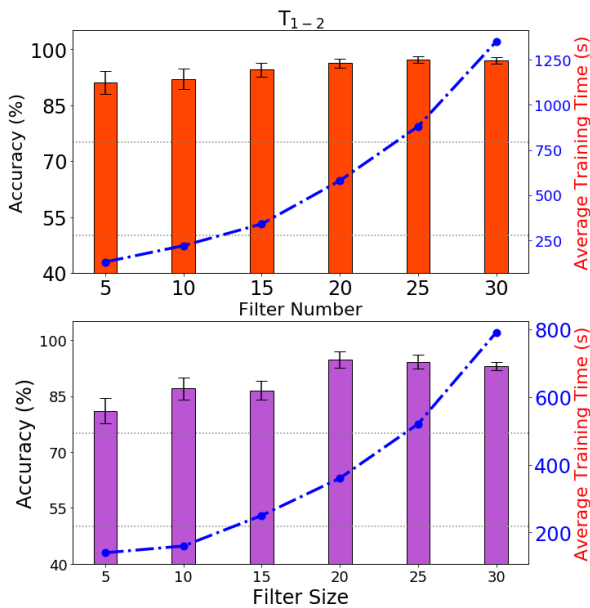


Figure 9. Impact of filter size and filter number on the testing accuracy for task  $T_{1-2}$ .

prediction uncertainty (measured by the standard deviation) reduces significantly. The proposed CNN-based domain adaptation method provides acceptable testing accuracy even with small training source samples,  $N_{source}$ .

As presented in Figure 11, the achieved testing accuracy in some tasks like  $T_{1-2}$  and  $T_{4-3}$  is higher than other tasks. This observation is due to the nature of data and the similarity between the distribution of source and target domain. For instance, the load variation from experiment #1 to experiment #2 is 40% which is smaller than that between experiment #1 and experiment #4 (i.e. 100%). Therefore, the transfer of learned features from experiment #1 to experiment #2 is easier. In addition, achieving the high accuracies in different tasks from low to high operational loads and vice versa indicates that the proposed method performs well bidirectional between different domains. The achieved results for different tasks also clearly illustrate the effectiveness of the motor current measurement signal for cross-domain fault diagnosis. As presented, by increasing

		Confusion Matrix					
Output Class	Chipped tooth	300 20.0%	0 0.0%	0 0.0%	0 0.0%	0 0.0%	100% 0.0%
	Eccentricity	0 0.0%	288 19.2%	0 0.0%	33 2.2%	0 0.0%	89.7% 10.3%
	Healthy	0 0.0%	0 0.0%	300 20.0%	0 0.0%	0 0.0%	100% 0.0%
	Missing tooth	0 0.0%	12 0.8%	0 0.0%	267 17.8%	0 0.0%	95.7% 4.3%
	Pitting	0 0.0%	0 0.0%	0 0.0%	0 0.0%	300 20.0%	100% 0.0%
		100% 0.0%	96.0% 4.0%	100% 0.0%	89.0% 11.0%	100% 0.0%	97.0% 3.0%
		Chipped tooth	Eccentricity	Healthy	Missing tooth	Pitting	Target Class

Figure 10. The confusion matrix for the classification results in task  $T_{1-2}$ .

the number of training samples, the diagnosis performance improves as well which follows the same pattern as the classical fault diagnosis methods.

**Classification Results and Comparison** Performance of the proposed transfer learning methodology is compared with two groups of fault diagnosis tools as summarized below:

Group A- Supervised classification methods such as:

1. LDA<sup>36</sup> - Linear Discriminant Analysis is a supervised algorithm that uses a linear transformation matrix to project features from parametric space to feature space.
2. SVM<sup>37</sup> - Support Vector Machines are supervised machine learning algorithms that can be employed for both regression and classification problems. SVMs are designed based on Structural Risk Minimization criteria in the statistical learning theory. SVMs work on a simple idea: to identify a hyper-plane which separates the training data into two distinct classes.
3. CNN Without Domain Adaptation (No-DA) - A deep learning method that automatically extracts

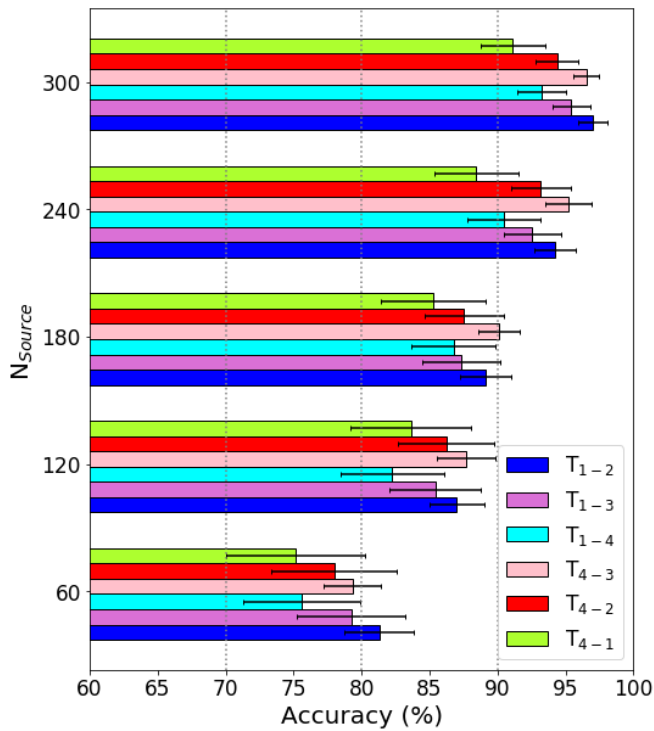


**Figure 11.** Performance of the proposed method at different tasks and for different training sample size.

features from the raw signal measurement. A typical classification is obtained by only considering the classification loss in Equation (5). This trained model is directly used for testing on the target dataset.

Group B- Transfer learning methods including:

1. TCA<sup>38</sup> - Transfer Component Analysis is used to find a feature subspace in the domain adaptation field. In the subspace created by transfer components, the source and target data distribution are similar. When the subspace is created, a SVM classifier is trained with the labeled source domain dataset and acquire the accuracy of the target domain.
2. JDA<sup>39</sup> - Joint Distribution Adaptation is a modification of TCA. It is able to simultaneously adapt the conditional and marginal distributions during the dimensionality reduction process.
3. GFK<sup>40</sup> - Geodesic Flow Kernel is an unsupervised domain adaptation technique wherein the source and target domain data are projected into a linear subspace while the shortest line path connects the two original domains.
4. BDA<sup>41</sup> - Balanced Distribution Adaptation aims to automatically balance the significance of marginal and conditional distribution discrepancies and therefore it can effectively adjust for a specific transfer task.
5. T-S<sup>42</sup> - This method suggests performing adaptation by learning a target-specific network from the source-specific network.

In Group A, three classification methods are used to learn representative features from the training source data in a supervised process and then the trained classifier is used on

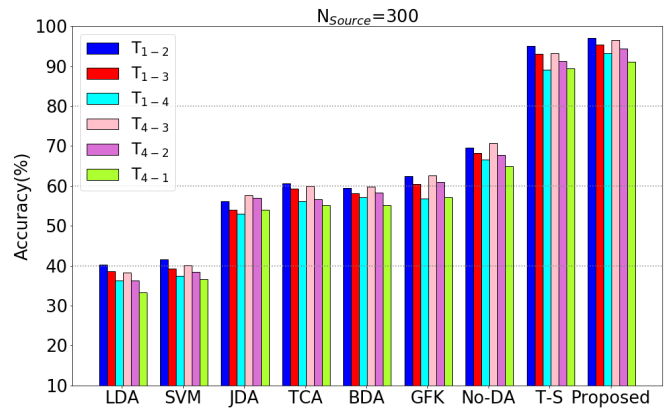


**Figure 12.** The achieved testing accuracy for different comparative methods and in all six transfer tasks.

the target domain data for testing and the achieved results are reported. Hand-crafted time and frequency domain features such as standard deviation, mean, peak to peak, kurtosis, frequency amplitude and energy *etc.* are used as an input to LDA and SVM methods. For No-DA, raw frequency-domain data is utilized. Because these methods inherently do not consider domain variation between the source and target datasets, therefore a low classification performance is highly expected. In Group B, the extracted time and frequency features are used for domain adaption tasks and the achieved results are compared with the proposed method.

Analyses are conducted on 300 samples obtained from the source and target dataset and the obtained diagnosis results on the testing (target domain) data are visualized in Figure 12. In contrast with other methods, the proposed approach provides the highest accuracies in all six transfer tasks, and basically, the accuracies are higher than 91%, which illustrates the effectiveness of the proposed transfer learning approach. The average performance improvement for the proposed method is 57.46%, 55.68%, 39.3%, 36.62%, 35.87%, 34.5%, 26.67%, 2.75% compared with LDA, SVM, GFK, JDA, TCA, BDA, No-DA, and T-S. The second-best performance is obtained from T-S and No-DA is ranked in the third place. Overall, domain adaptation methods discussed in Group B outperform the classical diagnosis methods in group A but they are not as promising as the proposed method.

The performance of different diagnosis methods for the low number of training samples e.g.  $N_{source} = 60$  and  $N_{target} = 300$ , is illustrated in Figure 13. As expected, using low number of labeled data for training deteriorates the testing diagnosis accuracy for all evaluated methods. This observation is consistent with the previous studies conducted on deep learning methods that larger training data leads to a better diagnosis performance and transfer learning based diagnosis methods also follow this pattern. Moreover, comparing the results obtained from methods in Group A (without domain adaptation) with the diagnosis results obtained from methods in Group B and the proposed method, shows the significant impact of cross-domain adaptation on fault diagnosis performance. T-S which provides an alternative way for domain adaptation, shows good performance with large training sample size. However,

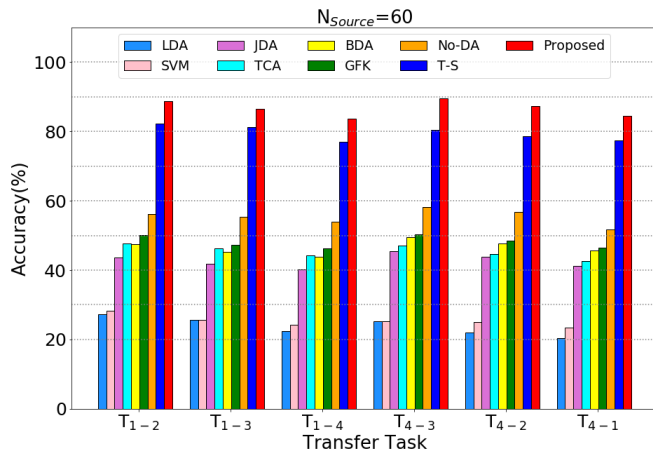


**Figure 13.** Fault diagnosis results with the low number of source domain samples in all six transfer tasks.

with a low sample size, its performance deteriorates significantly because this method minimizes the distribution discrepancy between the target dataset and the learned representations from the source training network. The achieved results illustrate the effectiveness of motor current signal for cross-domain fault diagnosis.

*Visualization of the learned features* In order to illustrate the effectiveness of our approach, T-distributed Stochastic Neighbor Embedding (t-SNE) technique is adapted in visualizing the high-level feature representation by mapping them from the original feature space into a 2-D space map. The visualization is performed on task  $T_{1-2}$  for the proposed method and also for CNN without domain adaptation (No-DA method). Figure 14 illustrates the virtualization of learned features in the fully connected layer of the source domain classifier without domain adaptation. As observed, without domain adaptation, samples from each identical class in the source or target data cluster together. However, for some labels there is a notable distribution discrepancy between the source and target domain samples. Since the feature space is divided into several regions associated with different labels, it is expected to obtain a low diagnosis performance in the target domain data. Therefore, it is necessary to bridge the distribution discrepancy between the source and target data to improve classification results on the target data.

By using domain adaptation, as is shown in Figure 14, the source and target domain features are projected into the same region as the model is trained. Accordingly, the distribution discrepancy has reduced significantly between the source and target domains and samples from different conditions are separated clearly. These two requirements a) minimal distribution discrepancy between two domains and b) clear differentiation between different health conditions in both domains would guarantee achieving an accurate cross-domain fault diagnosis. As illustrated, the cross-domain invariant features obtained by the proposed method are clustered well where features from different classes are separated clearly and only a small amount of overlapping is observed between classes ‘Eccentricity’ and ‘Missing tooth’ faults in the source and target domains.

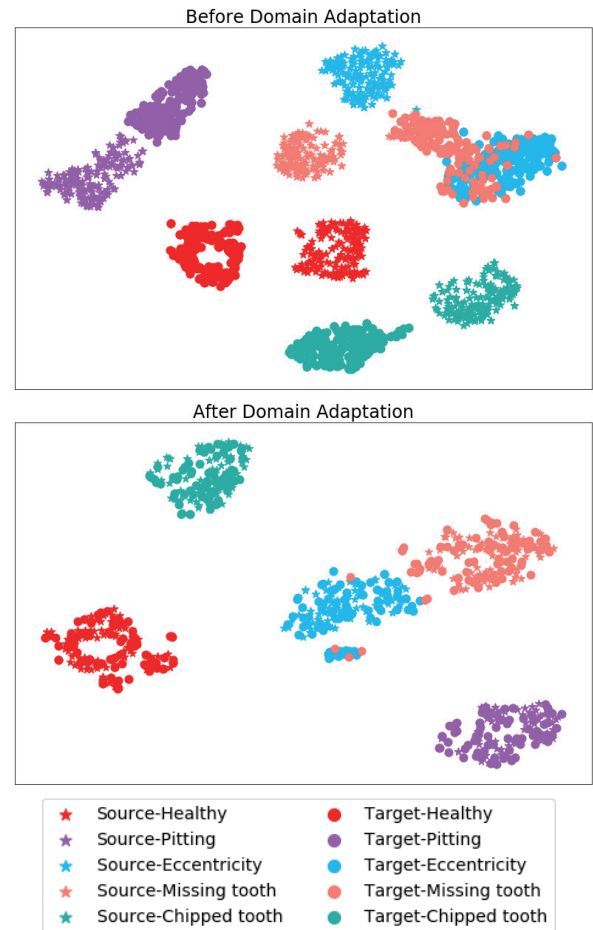


**Figure 14.** Extracted features in the fully connected layer are visualized for task  $T_{1-2}$  at  $N_{source} = 300$ . Both the scenarios before and after domain adaptation are presented.

## Conclusion

In this paper, a deep learning-based domain adaptation fault diagnostic method for gearboxes is proposed. An end-to-end diagnostic model is established, which takes the raw motor current data as inputs, and directly outputs the predicted health conditions. The maximum mean discrepancy metric is used to bridge the distribution gap between different gearbox operating conditions. Experiments on a real-world gearbox condition monitoring dataset are carried out for validations, and promising cross-domain fault diagnosis performance is achieved by the proposed domain adaptation method. This study offers a new perspective on enhancing fault diagnosis model generalization ability in different operating scenarios of gearboxes. The high data requirement of vibration signals by most existing methods is also alleviated, and effective diagnostic performance can be obtained using only the easily-collected current data.

However, it should be pointed out that the main limitation of this study lies in the assumption of the target-domain data during training. Further research works will be carried out on developing robust fault diagnosis models for different scenarios without the availability of the target-domain data in advance.

## References

1. Liu Y, Zhang J, Qin K et al. Diesel engine fault diagnosis using intrinsic time-scale decomposition and multistage Adaboost relevance vector machine. *Proceedings of the Institution of Mechanical Engineers, Part C: Journal of Mechanical Engineering Science* 2017; 232(5): 881–894.
2. Feng Y, Lu B and Zhang D. Multiscale morphological manifold for rolling bearing fault diagnosis. *Proceedings of the Institution of Mechanical Engineers, Part C: Journal of Mechanical Engineering Science* 2016; 231(19): 3516–3529.
3. Kia SH, Henao H and Capolino G. Torsional vibration assessment using induction machine electromagnetic torque estimation. *IEEE Transactions on Industrial Electronics* 2010; 57(1): 209–219.
4. Zhao D, Liu S, Gu D et al. Enhanced data-driven fault diagnosis for machines with small and unbalanced data based on variational auto-encoder. *Measurement Science and Technology* 2019; 31(3): 035004.
5. Lee J, Azamfar M and Singh J. A blockchain enabled cyber-physical system architecture for Industry 4.0 manufacturing systems. *Manufacturing Letters* 2019; 20: 34–39.
6. Azamfar M, Jia X, Pandhare V et al. Detection and diagnosis of bottle capping failures based on motor current signature analysis. *"Procedia Manufacturing"* 2019; 34: 840–846.
7. Yang D, Liu Y, Li S et al. Gear fault diagnosis based on support vector machine optimized by artificial bee colony algorithm. *Mechanism and Machine Theory* 2015; 90: 219–229.
8. Jia F, Lei Y, Lin J et al. Deep neural networks: A promising tool for fault characteristic mining and intelligent diagnosis of rotating machinery with massive data. *Mechanical Systems and Signal Processing* 2016; 72-73: 303–315.
9. Li X, Ding Q and Sun JQ. Remaining useful life estimation in prognostics using deep convolution neural networks. *Reliability Engineering & System Safety* 2018; 172: 1–11.
10. Guo X, Chen L and Shen C. Hierarchical adaptive deep convolution neural network and its application to bearing fault diagnosis. *Measurement* 2016; 93: 490–502.
11. Guo M, Yang N and Chen W. Deep-learning-based fault classification using Hilbert-Huang transform and convolutional neural network in power distribution systems. *IEEE Sensors Journal* 2019; 19(16): 6905–6913.
12. Chen Z, Li C, Sanchez R et al. Gearbox fault identification and classification with convolutional neural networks. *Shock and Vibration* 2015; 2015: 10.
13. Cheng F, Wang J, Qu L et al. Rotor-current-based fault diagnosis for DFIG wind turbine drivetrain gearboxes using frequency analysis and a deep classifier. *IEEE Transactions on Industry Applications* 2018; 54(2): 1062–1071.
14. Li C, Sanchez RV, Zurita G et al. Gearbox fault diagnosis based on deep random forest fusion of acoustic and vibratory signals. *Mechanical Systems and Signal Processing* 2016; 76-77: 283–293.
15. Csurka G. Domain adaptation for visual applications: A comprehensive survey. *arXiv preprint arXiv:170205374* 2017; .
16. Li X, Zhang W, Xu N et al. Deep learning-based machinery fault diagnostics with domain adaptation across sensors at different places. *IEEE Transactions on Industrial Electronics* 2019; : 1–1.
17. Liu Z, Lu B, Wei H et al. Fault diagnosis for electromechanical drivetrains using a joint distribution optimal deep domain adaptation approach. *IEEE Sensors Journal* 2019; : 1–1.
18. Li X, Zhang W, Ding Q et al. Multi-layer domain adaptation method for rolling bearing fault diagnosis. *Signal Processing* 2019; 157: 180–197.
19. Li X, Zhang W and Ding Q. A robust intelligent fault diagnosis method for rolling element bearings based on deep distance metric learning. *Neurocomputing* 2018; 310: 77–95.
20. Lu W, Liang B, Cheng Y et al. Deep model based domain adaptation for fault diagnosis. *IEEE Transactions on Industrial Electronics* 2017; 64(3): 2296–2305.
21. Hasan MJ, Islam MMM and Kim JM. Acoustic spectral imaging and transfer learning for reliable bearing fault diagnosis under variable speed conditions. *Measurement* 2019; 138: 620–631.
22. Cao P, Zhang S and Tang J. Preprocessing-free gear fault diagnosis using small datasets with deep convolutional neural network-based transfer learning. *IEEE Access* 2018; 6: 26241–26253.
23. Guo L, Lei Y, Xing S et al. Deep convolutional transfer learning network: A new method for intelligent fault diagnosis of machines with unlabeled data. *IEEE Transactions on Industrial Electronics* 2018; : 1–1.
24. Li X, Zhang W, Ding Q et al. Diagnosing rotating machines with weakly supervised data using deep transfer learning. *IEEE Transactions on Industrial Informatics* 2019; : 1–1.
25. Sharma V and Parey A. A review of gear fault diagnosis using various condition indicators. *Procedia Engineering* 2016; 144: 253–263.
26. Liu R, Yang B, Zio E et al. Artificial intelligence for fault diagnosis of rotating machinery: A review. *Mechanical Systems and Signal Processing* 2018; 108: 33–47.
27. Qiao W and Lu D. A survey on wind turbine condition monitoring and fault diagnosis - part II: Signals and signal processing methods. *IEEE Transactions on Industrial Electronics* 2015; 62(10): 6546–6557.
28. Mohanty AR and Kar C. Fault detection in a multistage gearbox by demodulation of motor current waveform. *IEEE Transactions on Industrial Electronics* 2006; 53(4): 1285–1297.
29. Lu D, Gong X and Qiao W. Current-based diagnosis for gear tooth breaks in wind turbine gearboxes. In *Proceedings of IEEE Energy Conversion Congress and Exposition (ECCE)*. pp. 3780–3786.
30. Singh S, Kumar A and Kumar N. Motor current signature analysis for bearing fault detection in mechanical systems. *Procedia Materials Science* 2014; 6: 171–177.
31. Salamon J and Bello JP. Deep convolutional neural networks and data augmentation for environmental sound classification. *IEEE Signal Processing Letters* 2017; 24(3): 279–283.
32. Shao S, McAleer S, Yan R et al. Highly-accurate machine fault diagnosis using deep transfer learning. *IEEE Transactions on Industrial Informatics* 2018; : 1–1.
33. Gretton A, Sejdinovic D, Strathmann H et al. *Optimal kernel choice for large-scale two-sample tests*. Curran Associates, Inc., 2012.
34. Li Y, Swersky K and Zemel R. Generative moment matching networks. In *Proceedings of 32nd International Conference on*

- Machine Learning*. pp. 1718–1727.
35. Li Z, Yan X, Tian Z et al. Blind vibration component separation and nonlinear feature extraction applied to the nonstationary vibration signals for the gearbox multi-fault diagnosis. *Measurement* 2013; 46(1): 259–271.
  36. Bandos TV, Bruzzone L and Camps-Valls G. Classification of hyperspectral images with regularized linear discriminant analysis. *IEEE Transactions on Geoscience and Remote Sensing* 2009; 47(3): 862–873.
  37. Ziani R, Felkaoui A and Zegadi R. Bearing fault diagnosis using multiclass support vector machines with binary particle swarm optimization and regularized Fisher's criterion. *Journal of Intelligent Manufacturing* 2017; 28(2): 405–417.
  38. Pan SJ, Tsang IW, Kwok JT et al. Domain adaptation via transfer component analysis. *IEEE Transactions on Neural Networks* 2011; 22(2): 199–210.
  39. Long M, Wang J, Ding G et al. Transfer feature learning with joint distribution adaptation. *Proceedings of the 2013 IEEE International Conference on Computer Vision* 2013; : 2200–2207.
  40. Gong B, Shi Y, Sha F et al. Geodesic flow kernel for unsupervised domain adaptation. In *Proceedings of IEEE Conference on Computer Vision and Pattern Recognition*. pp. 2066–2073.
  41. Wang J, Chen Y, Hao S et al. Balanced distribution adaptation for transfer learning. In *Proceedings of IEEE International Conference on Data Mining (ICDM)*. pp. 1129–1134.
  42. Tzeng E, Hoffman J, Saenko K et al. Adversarial discriminative domain adaptation. In *Proceedings of IEEE Conference on Computer Vision and Pattern Recognition (CVPR)*. pp. 2962–2971.